THE JOURNAL OF BIOLOGICAL CHEMISTRY VOL. 286, NO. 16, pp. 14670–14680, April 22, 2011

The Heparin-binding Domain of IGFBP-2 Has Insulin-like Growth Factor Binding-independent Biologic Activity in the Growing Skeleton*[S]

Received for publication, October 12, 2010, and in revised form, January 30, 2011 Published, JBC Papers in Press, March 3, 2011, DOI 10.1074/jbc.M110.193334

Masanobu Kawai[‡§], Anne C. Breggia[‡], Victoria E. DeMambro[‡], Xinchun Shen[¶], Ernesto Canalis[‖], Mary L. Bouxsein[**], Wesley G. Beamer[‡‡], David R. Clemmons[¶], and Clifford J. Rosen[‡1]

From the [‡]Center for Clinical and Translational Research, Maine Medical Center Research Institute, Scarborough, Maine 04074, the [§]Department of Bone and Mineral Research, Osaka Medical Center and Research Institute for Maternal and Child Health, Izumi, Osaka 594-1101, Japan, the [¶]Department of Medicine, University of North Carolina, School of Medicine, Chapel Hill, North Carolina 27599, the [‖]Department of Research, Saint Francis Hospital & Medical Center, Hartford, Connecticut 06105, the [**]Orthopaedic Biomechanics Laboratory, Beth Israel Deaconess Medical Center and Harvard Medical School, Boston, Massachusetts 02215, and [‡‡]The Jackson Laboratory, Bar Harbor, Maine 04609

Insulin-like growth factor-binding protein 2 (IGFBP-2) is a member of a family of six highly conserved IGFBPs that are carriers for the insulin-like growth factors (IGFs). IGFBP-2 levels rise during rapid neonatal growth and at the time of peak bone acquisition. In contrast, *Igfbp2*$^{-/-}$ mice have low bone mass accompanied by reduced osteoblast numbers, low bone formation rates, and increased PTEN expression. In the current study, we postulated that IGFBP-2 increased bone mass partly through the activity of its heparin-binding domain (HBD). We synthesized a HBD peptide specific for IGFBP-2 and demonstrated *in vitro* that it rescued the mineralization phenotype of *Igfbp2*$^{-/-}$ bone marrow stromal cells and calvarial osteoblasts. Consistent with its cellular actions, the HBD peptide *ex vivo* stimulated metacarpal periosteal expansion. Furthermore, administration of HBD peptide to *Igfbp2*$^{-/-}$ mice increased osteoblast number, suppressed marrow adipogenesis, restored trabecular bone mass, and reduced bone resorption. Skeletal rescue in the *Igfbp2*$^{-/-}$ mice was characterized by reduced PTEN expression followed by enhanced Akt phosphorylation in response to IGF-I and increased β-catenin signaling through two mechanisms: 1) stimulation of its cytosolic accumulation and 2) increased phosphorylation of serine 552. We conclude that the HBD peptide of IGFBP-2 has anabolic activity by activating IGF-I/Akt and β-catenin signaling pathways. These data support a growing body of evidence that IGFBP-2 is not just a transport protein but rather that it functions coordinately with IGF-I to stimulate growth and skeletal acquisition.

Insulin-like growth factor-binding protein-2 (IGFBP-2)[2] is a member of a highly conserved family of six IGFBPs that circulate or reside locally in the extracellular space including the bone marrow microenvironment (1–3). IGFBP-2 has high affinity for IGF-I/IGF-II and is believed to regulate IGF bioavailability in the pericellular environment. IGFBP-2 is the second most abundant circulating IGFBPs and is expressed in several mammalian tissues including the skeleton (2). Growing evidence demonstrates that increased IGFBP-2 levels are associated with reduced adipose tissue mass and improved glucose metabolism both in human and mouse models (4–6). Hedbacker *et al.* (5) recently reported that IGFBP-2 exhibits acute glucose lowering properties in several diabetic mouse models and that IGFBP-2 may mediate some of the metabolic activity of leptin. However, the role of IGFBP-2 in skeletal homeostasis is less clear and is dependent on the experimental model system. Generally, IGFBP-2 has been shown to inhibit IGF-I actions *in vitro* (3). Also, overexpression of *Igfbp2* inhibits growth hormone-stimulated chondrocytic expansion in growth hormone transgenic mice (7). However, Khosla and co-workers (8, 9) reported that IGFBP-2 markedly stimulated bone formation in patients with hepatitis C-associated osteosclerosis, and the administration of IGFBP-2 + IGF-II prevented bone loss in immobilized rats. Furthermore, we recently showed that *Igfbp2*$^{-/-}$ mice had markedly impaired bone formation, reduced trabecular bone volume fraction, and altered microarchitecture and low bone turnover, suggesting that IGFBP-2 might be extremely important within the skeletal milieu (10).

In addition to its IGF-I binding dependent actions, IGFBP-2 and other IGFBPs have been shown to stimulate biologic responses that are independent of their abilities to bind to IGFs (3). Similarly Lodish and co-workers (11) recently demonstrated that IGFBP-2 alone could stimulate hematopoietic stem cells *ex vivo*, although the mechanism of its action was not described. Previously, IGFBP-2 was reported to bind to extracellular matrices (12, 13). More recently several lines of evidence show that the heparin-binding domain (HBD) plays a

* This work was supported, in whole or in part, by National Institutes of Health Grant AR021707 (to E. C.) and National Institutes of Arthritis, Musculoskeletal, and Skin Disorders Grant AR153853 (to C. J. R.).

[S] The on-line version of this article (available at http://www.jbc.org) contains supplemental Tables S1 and S2 and Figs. S1–S3.

[1] To whom correspondence should be addressed: Maine Medical Center Research Institute, 81 Research Dr., Scarborough, ME 04074-7205. Tel.: 207-885-8100; Fax: 207-885-8174; E-mail: ROSENC@mmc.org.

[2] The abbreviations used are: IGFBP, insulin-like growth factor-binding protein; ALP, alkaline phosphatase; PPAR-γ, peroxisome proliferator-activated receptor-γ; HBD, heparin-binding domain; BMSC, bone marrow stromal cell; COB, calvarial osteoblast; αMEM, α-minimum essential medium; PEG-HBD, pegylated HBD; aBMD, areal bone mineral density; BrdUrd, bromodeoxyuridine; BW, body weight; aBMC, areal bone mineral content; PTEN, phosphatase and tensin homolog.

role in IGFBP-2 function. Russo *et al.* (14) reported that IGFBP-2 was proteolytically cleaved and that smaller fragments that include HBD still possessed the capacity to bind to extracellular matrix and with low affinity to IGF-I. They also demonstrated that IGFBP-2 stimulated the proliferation and metastatic behavior of neuroblastoma cells through the HBD (15). Interestingly, zebrafish IGFBP-2 lacks the HBD and cannot bind to any extracellular matrix (16). Taken together, these results suggest that IGFBP-2 binding to extracellular matrix is likely to be dependent on the HBD.

PTEN (phosphatase and tensin homolog deleted on chromosome 10) is a lipid phosphatase that opposes IGF-I signaling by dephosphorylating phosphatidylinositol 3,4,5-trisphosphate to phosphatidylinositol 4,5-diphosphate (17). Mice lacking PTEN only in osteoblasts showed progressively increasing bone mass with age, indicating the important role of PTEN and the PI3K/Akt signaling pathway in bone maintenance (18). There is also a negative correlation between IGFBP-2 and PTEN expression in certain types of tumor cells (19–21). Moreover, we reported that PTEN expression was enhanced in osteoblasts derived from *Igfbp2*$^{-/-}$ bone marrow stromal cells (10). Interestingly, Perks *et al.* (20) suggested that IGFBP-2 suppression of PTEN was mediated in an IGF binding-independent manner. Because Akt activation is a critical factor regulating bone mass (22, 23), we speculated that IGFBP-2 could enhance Akt signaling by suppressing PTEN expression independent of IGF-I binding and that the HBD is involved in the down-regulation of PTEN.

IGFBP-2 contains two putative HBDs: one HBD in the C terminus domain shares the sequence similarity with other HBD containing IGFBPs such as IGFBP-3 and IGFBP-5 (3). On the other hand, the HBD in the linker region is unique and is not present in other IGFBPs. Based on the unique sequence of the IGFBP-2 HBD subsequently referred to simply as the HBD, we generated a peptide corresponding to the one in the linker region and tested whether the HBD peptide affected skeletal turnover. We found that the HBD peptide has an anabolic effect on the skeleton through suppression of PTEN in osteoblasts and that this effect was mediated by enhanced Akt and β-catenin signaling. Moreover, there was significant synergy between the HBD and IGF-I in respect to enhancement of pAKT and β-catenin production.

EXPERIMENTAL PROCEDURES

Mice—Generation of the original mixed background strain B6;129-*Igfbp2*<*tm1Jep*>, which we refer to as *Igfbp2*$^{-/-}$ mice, has been described previously (10, 24). The original mice were backcrossed onto C57BL/6J background for 10 generations. *Igfbp2*$^{+/+}$ mice were C57BL/6J controls. All of the experimental studies were performed with male mice. All of the animal studies were reviewed and approved by the Institutional Animal Care and Use Committee of Maine Medical Center Research Institute.

Cell Culture—MC3T3-E1 cells were purchased from ATCC and maintained in αMEM containing 10% FCS neonatal calvarial osteoblasts were collected from 7–10-day-old mice. Briefly, calvariae were digested five times with collagenase P and trypsin. The cells released from digests 2–5 were collected as primary calvarial osteoblasts and maintained in DMEM supplemented with 10% FCS and nonessential amino acids. Osteoblastogenesis of primary calvarial osteoblasts was analyzed by treating cells with 4 mM of β-glycerophosphate and 50 μg/ml of ascorbic acid in αMEM with 10% FCS. Bone marrow stromal cells (BMSCs) were harvested from femurs and tibias of 8-week-old mice. BMSCs were grown in αMEM containing 10% FCS. Osteoblastogenesis of BMSCs was induced by the treatment with osteogenic medium consisting of αMEM containing 10% FCS, 8 mM β-glycerophosphate, and 50 μg/ml ascorbic acid.

Metacarpal Culture—Metacarpals were isolated from *Igfbp2*$^{-/-}$ mice from 1-day-old mice and incubated in DMEM containing 0.5% BSA, 50 μg/ml ascorbic acid, and 1 mM β-glycerol phosphate for 10 days. Stimulants were added to culture medium from day 1. At day 10, metacarpals were incubated in medium containing calcein (500 ng/ml) for 2 h for staining of calcium deposition, and images were obtained. The bones were then fixed with 4% phosphonoformic acid, embedded in paraffin, and processed for Alcian blue and von Kossa double staining.

Real Time RT-PCR—Total RNA was prepared using a RNeasy mini kit (Qiagen). cDNA was generated using a random hexamer and reverse transcriptase (Superscript III; Invitrogen) according to the manufacturer's instructions. Quantification of mRNA expression was carried out using an iQ SYBR Green Supermix in a iQ5 thermal cycler and detection system (Bio-Rad). GAPDH was used as an internal standard control gene for all quantification. The primer sequences are available upon request.

Western Blot Analysis—To prepare whole cell lysates, the cells were solubilized in radioimmune precipitation assay buffer (50 mM Tris, 150 mM NaCl, 1 mM EDTA, 1% Nonidet P-40, 0.25% sodium deoxycholate, 2 μg/ml aprotinin, 2 μg/ml leupeptin, 2 μg/ml pepstatin A, 0.5 mM phenylmethylsulfonyl fluoride, and 1 mM dithiothreitol). To isolate the cytosolic fraction, the cells were solubilized with hypotonic buffer containing protease and phosphatase inhibitors (10 mM Tris, 0.2 mM $MgCl_2$, pH 7.4) and kept on ice for 10 min. The cell lysates were mixed with sucrose buffer (final concentrations: 25 mM sucrose, 0.1 mM EDTA) and centrifuged at 20,000 × *g* for 1 h. The supernatant contained the cytosolic fraction. To prepare the membrane fraction, the cells were solubilized with PBS containing protease and phosphatase inhibitors. The lysates were frozen at −80 °C for 1 h and thawed at room temperature. After three cycles, they were centrifuged at 13,000 × *g* for 25 min. The pellet was resuspended with membrane protein isolation buffer (20 mM Tris-HCl, 150 mM NaCl, 1 mM EDTA, 1 mM EGTA, and 1% Triton X-100, pH 7.5) containing protease and phosphatase inhibitors. Equal amounts of sample were separated by SDS-PAGE and transferred electrophoretically to nitrocellulose membranes. The membranes were blocked in 5% BSA in Tris-buffered saline. Thereafter, the membranes were immunoblotted with anti-PTEN (Cell Signaling), anti-Akt (Cell Signaling), anti-Ser(P)^{473}-Akt (Cell Signaling), anti-β-catenin (BD Transduction Laboratories, 610153), anti-Ser(P)^{552}-β-catenin (Cell Signaling), or anti-β-actin (Santa Cruz) and developed with horseradish peroxidase-coupled anti-mouse or rabbit IgG

antibodies, followed by enhancement with SuperSignal West Dura extended duration substrate antibodies (Pierce).

Immunoprecipitation with Akt1 and Akt2—The cells were starved with serum-free medium overnight and then exposed to 0 or 50 ng/ml IGF-I for 10 min. The cells were lysed with radioimmune precipitation assay buffer. The cell lysates were centrifuged at 14,000 × *g* for 10 min at 4 °C. They were immunoprecipitated with either anti-Akt1 antibody (1:500) or anti-Akt2 antibody (1:500) overnight at 4 °C. The immunoprecipitates were immobilized using protein A-Sepharose beads for 2 h at 4 °C and washed three times with the same buffer. The precipitated proteins were eluted in 40 μl of 2× Laemmli sample buffer, boiled for 5 min, and separated using 10% SDS-PAGE. The proteins were then transferred to Immobilon-P membranes. The blots were incubated overnight at 4 °C with the indicated antibodies. The proteins were visualized using enhanced chemiluminescence (Pierce).

Generation of Heparin-binding Domain Peptide—The synthetic peptide containing the heparin-binding domain (amino acids 196–199) and nine additional amino acids of mouse IGFBP-2, ^{188}KHLSLEEPKKLRP^{200} (referred to as HBD peptide), and control peptide for HBD peptide (AALSLEEPAALAP) were synthesized by the Protein Chemistry Core Facility at the University of North Carolina. Purity and sequence confirmation were determined by mass spectrometry. The synthetic peptide for heparin-binding domain of IGFBP5 (^{201}RKGFYKRKQCKPSRGRKR^{218}) was also generated using the same method as mentioned above. The IGFBP-2-HBD peptide was pegylated as follows: 10 mg of peptide was mixed with 380 μg of methoxy PEG maleimide (20,000 kDa) (1:3 molar ratio peptide to PEG) (Jenkem Biotechnology) in 4.0 ml of 0.05 M $NaPO_4$, pH 7.0. Following an overnight incubation at 4 °C, cysteine was added to a final concentration of 17 mM to block untreated sites. To remove the nonpegylated peptide and cysteine, the mixture was desalted using a Zebra Desalt spin column (Thermo Scientific) following the manufacturer's instructions. Pegylation was verified by SDS-PAGE analysis with Coomassie staining.

In Vitro IGFBP-2 Binding Assay—The cells were starved with serum-free medium overnight and then exposed to 0 or 50 ng/ml IGF-I for 10 min. They were suspended in 100 μl of PBS (pH 7.4) and incubated with biotinylated BP2 (final concentration, 28 nM) and/or HBD (140 nM) for 4 h at 4 °C. The cells were washed three times with PBS and lysed with radioimmune precipitation assay buffer. The cell lysates were centrifuged at 14,000 × *g* for 10 min at 4 °C. The proteins from supernatants were separated by 12.5% of SDS-PAGE and detected using HRP-conjugated avidin.

In vivo treatment of Igfbp2$^{-/-}$ Mice with Pegylated (PEG) HBD Peptide—Igfbp2$^{-/-}$ mice were administered with PBS or PEG-HBD peptide (50 μg/day) intraperitoneally five times/week from 6 to 9 weeks of age. Dual energy x-ray absorptiometry was performed before the initiation of treatment. The mice were injected with 20 mg/kg calcein intraperitoneally 7 and 2 days before sample collection.

Dual Energy X-ray Absorptiometry—Dual energy x-ray absorptiometry for whole body and femoral areal bone mineral density (aBMD, g/cm^2) and body composition exclusive of the head were performed using the PIXImus (GE-Lunar) as described previously (10).

Micro-computed Tomography—Microarchitecture of distal trabecular bone and midshaft cortical bone were analyzed with femurs and vertebrae (L5) by high resolution microcomputed tomography (MicroCT40; Scanco Medical AG, Switzerland). Approximately 100 CT slices were measured just proximal to the distal growth plate, using an isotropic voxel size of 12 μm. Midshaft cortical bone properties were analyzed in a similar fashion using 18 CT slices obtained at the midfemoral diaphysis.

Bone Histomorphometry—In vivo histomorphometry differences were analyzed between *Igfbp2$^{-/-}$* mice treated with PBS or PEG-HBD peptide at 9 weeks of age. The mice were injected with 20 mg/kg calcein intraperitoneally 7 and 2 days before sample collection. The femurs were analyzed as described previously (10).

Femoral Biomechanics—Femoral biomechanical properties were compared by three-point bending between *Igfbp2$^{-/-}$* mice treated with PBS or PEG-HBD peptide at 9 weeks of age. Load was applied at a constant rate (0.05 mm/s) until failure. We measured maximum load (newtons), bending stiffness (newtons/mm), and work-to-failure (newtons/mm) from the load displacement curve and computed the apparent elastic modulus and ultimate strength using the relevant midfemoral cross-sectional geometry measured from microCT.

In Vivo BrdUrd Assay—BrdUrd (100 μg/g of BW) and FdU (12 μg/g of BW) were injected intraperitoneally in 2-week-old male mice. 2 h after of injection femurs were collected and fixed in 4% phosphonoformic acid overnight at 4 °C. The femurs were decalcified using 15% EDTA (pH 7.4) for 5 days and sectioned. Endogenous peroxidase was blocked with 0.3% H_2O_2 in PBS, and the sections were incubated with a mouse monoclonal anti-BrdUrd antibody (1:200; Sigma B8434) overnight at 4 °C. The sections were then incubated with a biotinylated goat anti-mouse secondary antibody followed by the incubation with streptavidin-biotinylated HRP complex and visualized with 3,3′-diaminobenzidine.

Statistical Analysis—All of the data are expressed as the means ± S.E. The results were analyzed for statistically significant differences using Student's *t* test or analysis of variance followed by Bonferroni multiple comparison *post hoc* test. Statistical significance was set at $p < 0.05$.

RESULTS

The Heparin-binding Domain of IGFBP-2 Stimulates in Vitro Osteoblastogenesis—Previously, we reported that male *Igfbp2$^{-/-}$* mice exhibited an osteopenic phenotype with low bone formation and that osteoblastogenesis was impaired in BMSCs from *Igfbp2$^{-/-}$* mice compared with wild-type cells. Interestingly, male *Igfbp2$^{-/-}$* mice have a profound reduction in osteoblast number that accounts for the reduction in bone volume fraction in the tibia and femur, although the percentage of osteoblast apoptosis by TUNEL staining did not differ between *Igfbp2$^{-/-}$* and *Igfbp2$^{+/+}$*. To investigate whether the HBD of IGFBP-2 could be responsible for the phenotype of the *Igfbp2$^{-/-}$* mouse, we generated a synthetic peptide (the HBD peptide) that does not bind IGFs and that contains the HBD of

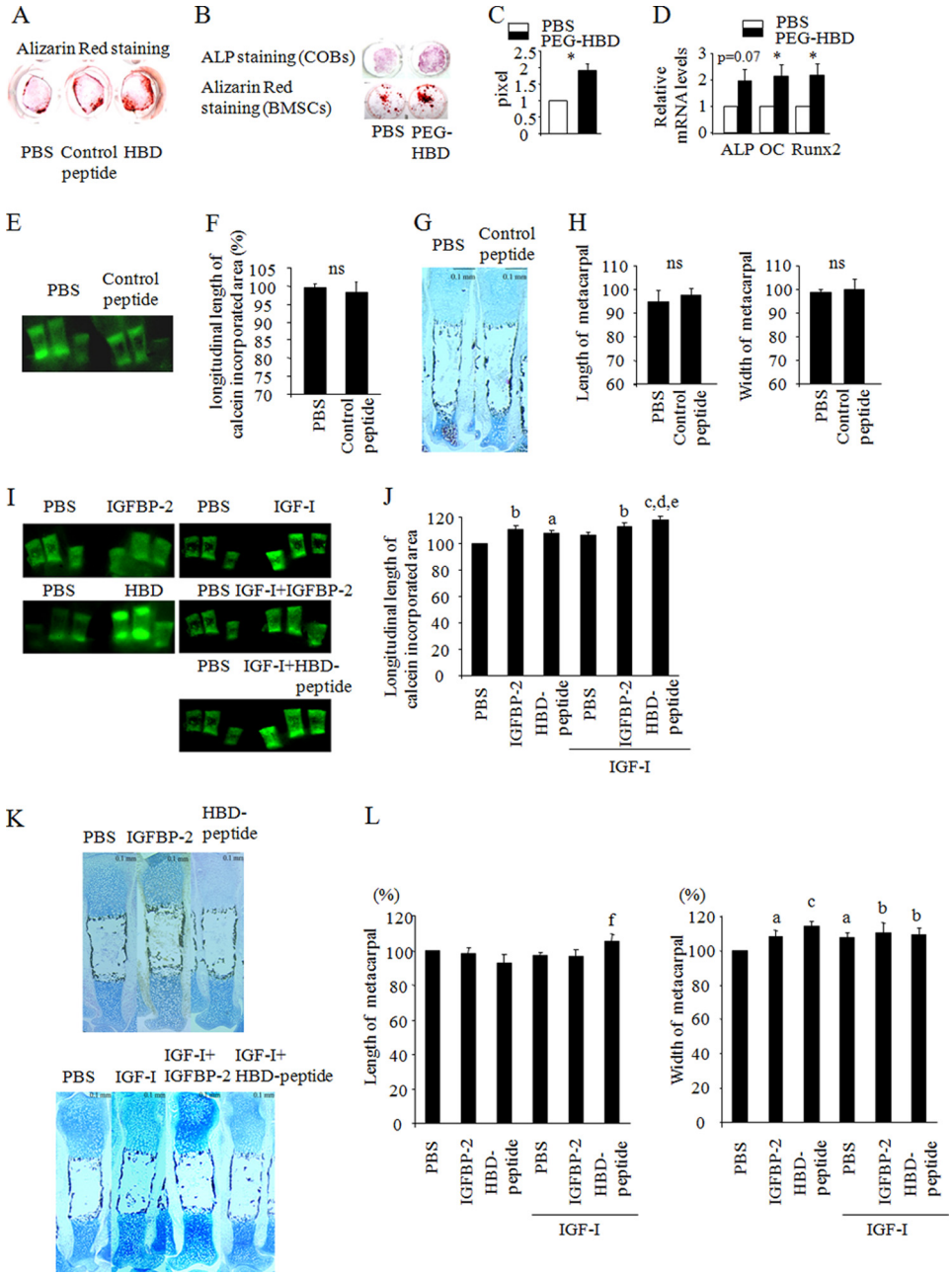

FIGURE 1. **The heparin-binding domain of IGFBP-2 enhances osteoblastogenesis *in vitro* and *ex vivo*.** *A*, *Igfbp2*$^{-/-}$ COBs were cultured with osteogenic medium with PBS, control peptide (2 μg/ml), or the HBD peptide (2 μg/ml). Osteoblastogenesis was evaluated by Alizarin Red staining. *B–D*, *Igfbp2*$^{-/-}$ COBs and BMSCs were treated with osteogenic medium with PEG-HBD peptide (2 μg/ml). ALP staining (day 7) and Alizarin Red staining (day 14) were performed (*B*). Alizarin Red staining positive area was quantified using NIH Image (*C*). Expression of *ALP*, *OC*, and *Runx2* was analyzed by real time RT-PCR using BMSCs at day 14 ($n = 3$) (*D*). *E–L*, *Igfbp2*$^{-/-}$ metacarpals were treated with osteogenic medium with PBS or control peptide (2 μg/ml) (*E–H*). *Igfbp2*$^{-/-}$ metacarpals were treated with osteogenic medium with IGFBP-2 (200 ng/ml) or the HBD peptide (2 μg/ml) in the presence or absence of IGF-1 (20 ng/ml) (*I–L*). At day 10, the bones were treated with 500 ng/ml of calcein for 2 h. The calcein-incorporated area was visualized (*E* and *I*), and the longitudinal length of the calcein-incorporated area was quantified (*F* and *J*). Metacarpals were fixed with 4% phosphonoformic acid and subjected to Alcian blue and von Kossa double staining (*G* and *K*). The length and width of the whole metacarpals were quantified (*H* and *L*). The figures shown represent at least three independent experiments. The values are expressed as the means ± S.E. ($n = 3–4$). *, $p < 0.05$; *a*, $p < 0.05$ *versus* PBS; *b*, $p < 0.01$ *versus* PBS; *c*, $p < 0.001$ *versus* PBS; *d*, $p < 0.01$ *versus* HBD peptide; *e*, $p < 0.05$ *versus* IGF-I; *f*, $p < 0.05$ *versus* HBD peptide; *ns*, not significant.

IGFBP-2, and tested its effect on osteoblastogenesis *in vitro*. To confirm the specificity of the HBD peptide, we also made a control peptide and analyzed its effect on osteogenesis. The control peptide did not enhance mineralization of *Igfbp2*$^{-/-}$ COBs compared with PBS-treated cells, whereas the HBD peptide stimulated COB mineralization (Fig. 1*A*). Based on this, PBS was used as controls for further studies. To prolong the half-life of the HBD peptide such that it was feasible to undertake *in vivo* studies, pegylation of the HBD peptide was performed (PEG-HBD). *Igfbp2*$^{-/-}$ COBs and BMSCs were cultured in osteogenic medium in the presence of PBS, the PEG-HBD peptide, or the HBD peptide. Both PEG-HBD and HBD peptide enhanced osteogenesis as measured by alkaline phosphatase and Alizarin Red staining (Fig. 1, *A–C*). Consistent

with this, *ALP*, *Runx2* (Runt-related transcription factor 2), and *OC* (osteocalcin) expression was enhanced in BMSCs treated with PEG-HBD- *versus* PBS-treated cells (Fig. 1*D*). Thus, there was no difference between the pegylated form of HBD and the HBD itself with respect to induction of osteogenesis.

The Heparin-binding Domain of IGFBP-2 Stimulates Periosteal Expansion of Metacarpals ex Vivo—To further understand the anabolic effect of HBD on the skeleton, we next collected metacarpals from 1-day-old mice, incubated them with osteogenic medium in the absence of fetal calf serum, and tested the effects of the HBD peptide on osteogenesis. Bone accrual was evaluated by the longitudinal length of the calcein-incorporated area as well as the width and length of the whole metacarpals. The control peptide had no effect on the calcein-incorporated area, and the length and width of the whole metacarpals were comparable with the metacarpals treated with PBS (Fig. 1, *E–H*). Hence PBS was used as the control for further studies. IGFBP-2 and the HBD peptide significantly enhanced the calcein-incorporated area of metacarpals (Fig. 1, *I* and *J*). IGF-I also stimulated expansion of the calcein-incorporated area to a similar extent as IGFBP-2 and the HBD peptide (Fig. 1, *I* and *J*). When metacarpals were treated with IGF-I together with the HBD peptide, the metacarpals displayed further enhancement of the calcein-incorporated area (Fig. 1, *I* and *J*). In addition, IGFBP-2 and HBD peptide also increased the width of the whole metacarpals, implying that IGFBP-2 has an important role in periosteal expansion (Fig. 1, *K* and *L*).

Because other IGFBPs possess HBD regions as well as IGFBP-2, we analyzed whether the osteogenic effect of the HBD is specific for this region in IGFBP-2 or whether the HBD in other forms of IGFBPs also had this effect. For this purpose, we prepared a peptide that contained the HBD region of IGFBP-5 (BP5-HBD) in which the amino acid sequence is quite similar to the HBD in the C-terminal region of IGFBP-2 and determined its effect on osteogenesis. We cultured *Igfbp2*-deficient COBs in the presence of BP5-HBD and found that BP5-HBD did not show any enhancement of differentiation or mineralization compared with PBS-treated cells (Fig. 2*A*). Second, we collected metacarpals and cultured them in osteogenic medium with or without BP5-HBD. BP5-HBD had no effect on the calcein-incorporated area, length, or width of whole metacarpals (Fig. 2, *B–E*). These data suggest that the effect of the HBD on skeletal acquisition is likely specific to IGFBP-2.

The HBD of IGFBP-2 Increases Bone Mass in Growing Igfbp2$^{-/-}$ *Mice*—Next, we tested whether the HBD peptide could enhance bone mass *in vivo*. After calculating the half-life of PEG-HBD (data not shown) *in vivo*, we administered 50 μg of PEG-HBD five times per week for 3 weeks to *Igfbp2* $^{-/-}$ mice starting at 6 weeks of age. Because administration of pegylated control peptide in female C57BL/6J mice did not show any difference in terms of the change in aBMD compared with the treatment with PBS, PBS was used as a control in the *in vivo* study (supplemental Fig. S1). We first analyzed whether PEG-HBD could reverse the bone loss observed in the *Igfbp2*$^{-/-}$ male mice. At base line, aBMD and areal bone mineral content (aBMC)/BW did not differ between *Igfbp2*$^{-/-}$ mice treated with PBS or PEG-HBD (supplemental Table S1). As expected, *Igfbp2*$^{+/+}$ mice treated with PBS had higher trabecular bone

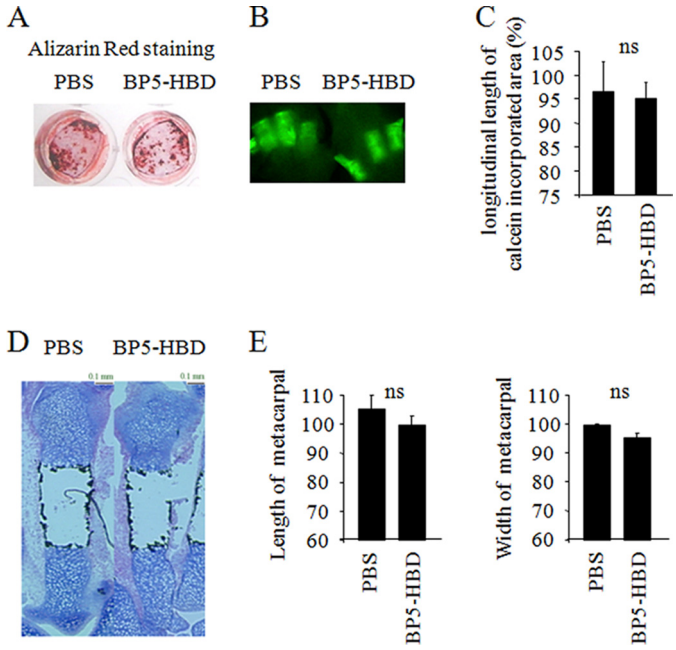

FIGURE 2. **The heparin-binding domain of IGFBP-5 does not show any effects on *in vitro* osteoblastogenesis or periosteal expansion of metacarpals *ex vivo*.** *A*, *Igfbp2*$^{-/-}$ primary calvarial osteoblasts were treated with osteogenic medium with or without the heparin-binding domain of IGFBP-5 (BP5-HBD) (2 μg/ml). Osteoblastogenesis was evaluated by Alizarin Red staining. *B–E*, *Igfbp2*$^{-/-}$ metacarpals were treated with osteogenic medium with or without BP5-HBD (2 μg/ml) for 10 days. The bones were labeled with calcein (500 ng/ml), and the calcein-incorporated area was visualized (*B*). The longitudinal length of calcein-incorporated area was quantified (*C*). Alcian blue and Von Kossa double staining was performed (*D*), and the length and width of whole metacarpals were quantified (*E*). The figures shown represent at least three independent experiments. The values are expressed as the means ± S.E. ($n = 3$). *ns*, not significant.

TABLE 1

MicroCT analysis of femurs from PBS-treated IGFBP2$^{+/+}$ and PBS or PEG-HBD peptide-treated IGFBP2$^{-/-}$ male mice

The values are expressed as the means ± S.E.

	PBS		PEG-HBD
	Igfbp2$^{+/+}$ ($n = 8$)	*Igfbp2*$^{-/-}$ ($n = 12$)	*Igfbp2*$^{-/-}$ ($n = 6$)
Midshaft			
Cortical thickness (mm)	0.198 ± 0.007	0.197 ± 0.003	0.200 ± 0.006
Bone area (mm^2)	0.889 ± 0.047	0.868 ± 0.018	0.903 ± 0.024
Total area (mm^2)	1.970 ± 0.062	1.955 ± 0.036	2.076 ± 0.031[b]
Bone area/total area	0.449 ± 0.011	0.444 ± 0.006	0.435 ± 0.014
Distal femur			
Bone volume/total volume	0.143 ± 0.017	0.095 ± 0.007[a]	0.125 ± 0.012[c]
Trabecular number (1/mm)	4.86 ± 0.16	4.29 ± 0.09[a]	4.47 ± 0.15
Trabecular thickness (mm)	0.047 ± 0.003	0.041 ± 0.001	0.048 ± 0.002[d]
Trabecular spacing (mm)	0.200 ± 0.007	0.230 ± 0.005[a]	0.221 ± 0.008

[a] $p < 0.01$ *versus* *Igfbp2*$^{+/+}$ with PBS.
[b] $p < 0.05$ *versus* *Igfbp2*$^{-/-}$ with PBS.
[c] $p < 0.05$ *versus* *Igfbp2*$^{-/-}$ with PBS.
[d] $p < 0.01$ *versus* *Igfbp2*$^{-/-}$ with PBS.

volume by microCT compared with PBS-treated *Igfbp2*$^{-/-}$ mice (Table 1). In *Igfbp2*$^{-/-}$ mice, 3 weeks of treatment with PEG-HBD enhanced aBMD and aBMC/BW compared with PBS, although it did not reach a statistical significance (supplemental Table S1). MicroCT revealed a higher trabecular bone volume fraction and greater trabecular thickness in both the distal femur and L5 vertebrae of *Igfbp2*$^{-/-}$ mice treated with PEG-HBD- *versus* PBS-treated *Igfbp2*$^{-/-}$ mice. (Fig. 3*A* and Tables 1 and 2). At the femoral midshaft, cortical thickness was not affected by PEG-HBD treatment, but total bone area was

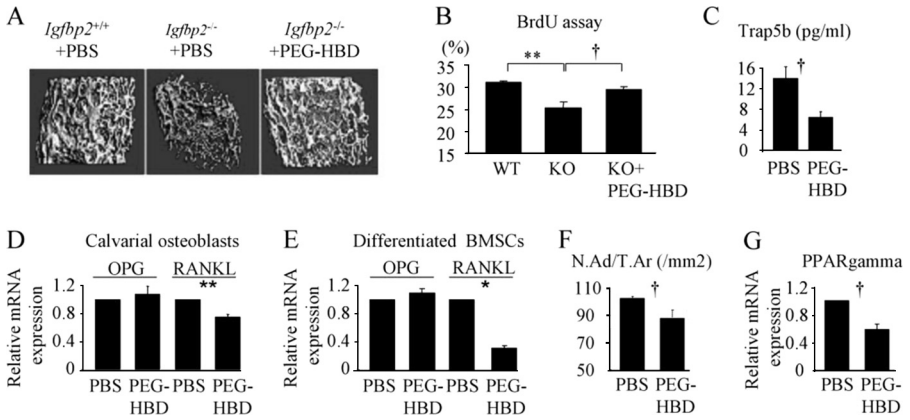

FIGURE 3. **The heparin-binding domain of IGFBP-2 enhances bone mass of *Igfbp2*$^{-/-}$ mice.** Male *Igfbp2*$^{+/+}$ mice were treated with PBS, and male *Igfbp2*$^{-/-}$ mice were treated with PBS or PEG-HBD domain from 6 to 9 weeks (*A*, *C*, and *F*). Two-week-old male *Igfbp2*$^{+/+}$ mice were treated with PBS, and *Igfbp2*$^{-/-}$ mice were treated with PBS or PEG-HBD (15 μg) for 3 days (*B*). *A*, microCT image of distal femur at 9 weeks old. *B*, BrdUrd staining was performed using the distal femur, and the percentage of BrdUrd positive osteoblasts was calculated ($n = 3$). *C*, serum Trap5b levels were analyzed by ELISA in *Igfbp2*$^{-/-}$ mice at 9 weeks old ($n = 6$–9). *D*, *Igfbp2*$^{-/-}$ COBs were treated with or without PEG-HBD for 2 h. *E*, *Igfbp2*$^{-/-}$ BMSCs were cultured with osteogenic medium with PBS or PEG-HBD for 2 weeks. Expression of *Opg* and *Rankl* was analyzed by real time RT-PCR ($n = 3$). *F*, adipocyte number was counted just proximal to the distal growth plate of femur and normalized by the total area (*N.Ad/T.Ar*) in *Igfbp2*$^{-/-}$ mice at 9 weeks old ($n = 6$). *G*, *Igfbp2*$^{-/-}$ COBs were treated with PBS or PEG-HBD for 24 h in serum-free medium. Expression of *Pparg* was analyzed by real time PCR ($n = 3$). The figures shown represent at least three independent experiments. The values are expressed as the means ± S.E. *, $p < 0.001$; **, $p < 0.01$; †, $p < 0.05$.

TABLE 2

MicroCT analysis of vertebrae (L5) from male *Igfbp2*$^{+/+}$ treated with PBS and male *Igfbp2*$^{-/-}$ treated with PBS or PEG-HBD

The values are expressed as the means ± S.E.

	PBS		PEG-HBD
	Igfbp2$^{+/+}$ ($n = 7$)	*Igfbp2*$^{-/-}$ ($n = 9$)	*Igfbp2*$^{-/-}$ ($n = 6$)
Bone volume/total volume	0.314 ± 0.020	0.278 ± 0.010	0.305 ± 0.012[a]
Trabecular number (1/mm)	6.15 ± 0.36	5.77 ± 0.11	5.70 ± 0.10
Trabecular thickness (mm)	0.052 ± 0.002	0.049 ± 0.001	0.054 ± 0.002[b]
Trabecular spacing (mm)	0.155 ± 0.009	0.160 ± 0.004	0.161 ± 0.004

[a] $p = 0.09$ *versus* *Igfbp2*$^{-/-}$ with PBS.
[b] $p < 0.05$ *versus* *Igfbp2*$^{-/-}$ with PBS.

TABLE 3

Histomorphometric analysis of femur from male *Igfbp2*$^{-/-}$ mice treated with PBS or PEG-HBD

The values are expressed as the means ± S.E. OS, osteoid surface; BS, bone surface; ObS, osteoblast surface; Nob, osteoblast number; BPm, bone perimeter; ES, erosion surface; OcS, osteoclast surface; Noc, osteoclast number; MAR, mineral apposition rate; BFR, bone formation rate.

	Igfbp2$^{-/-}$	
	PBS ($n = 5$)	PEG-HBD ($n = 5$)
OS/BS (%)	2.38 ± 1.11	3.56 ± 0.44
ObS/BS (%)	11.5 ± 1.03	16.26 ± 1.42[a]
Nob/BPm(/mm)	12.31 ± 0.52	16.3 ± 1.4[a]
ES/BS (%)	17.11 ± 0.93	14.79 ± 01.58
OcS/BS (%)	11.02 ± 0.87	9.14 ± 0.90
Noc/BPm (per mm)	5.19 ± 0.37	4.37 ± 0.39
MAR (μm/day)	0.873 ± 0.0078	0.91 ± 0.0453
Bone formation rate/surface/day ($\mu m^3/\mu m^2$/day)	0.0796 ± 0.0164	0.080 ± 0.0191

[a] $p < 0.05$ *versus* *Igfbp2*$^{-/-}$ with PBS.

increased in PEG-HBD-treated *Igfbp2*$^{-/-}$ mice *versus* PBS-treated *Igfbp2*$^{-/-}$ mice (Table 1). This is consistent with an effect of PEG-HBD on periosteal expansion that was also noted in the metacarpal assay. The cortical bone changes were associated with a modest albeit nonsignificant increase in strength parameters analyzed by a three-point bending assay (supplemental Fig. S2). In addition, 3 weeks of treatment with PEG-HBD did not have any effect on the width and morphology of growth plate, which is consistent with the *ex vivo* metacarpal culture findings that the HBD did not affect the length of whole metacarpals (supplemental Fig. S3).

Dynamic histomorphometry revealed that osteoblast number per bone perimeter was increased 33% in PEG-HBD-treated *Igfbp2*$^{-/-}$ mice *versus* PBS-treated *Igfbp2*$^{-/-}$ mice, whereas osteoclast number showed a trend toward a decrease in the PEG-HBD-treated *Igfbp2*$^{-/-}$ mice *versus* PBS-treated *Igfbp2*$^{-/-}$ mice (Table 3). Consistent with the increase in osteoblast number in HBD-treated mice, *in vivo* BrdUrd labeling of the femur in *Igfbp2* $^{-/-}$ mice revealed significantly enhanced proliferation of osteoblasts in the HBD-treated *Igfbp2*$^{-/-}$ group compared with PBS-treated *Igfbp2*$^{-/-}$ mice; furthermore the degree of BrdUrd labeling in the HBD-treated group was the same as that of PBS-treated *Igfbp2*$^{+/+}$ mice (Fig. 3*B*).

Consistent with the decreased number of osteoclasts, serum TRAP5b levels were significantly decreased in PEG-HBD-treated *Igfbp2*$^{-/-}$ mice (Fig. 3*C*). However, PEG-HBD or HBD peptide did not directly affect osteoclastogenesis in *Igfbp2*$^{-/-}$ bone marrow cells (data not shown), although PEG-HBD suppressed *Rankl* (receptor activator of NF-κB ligand) expression without changing *Opg* (osteoprotegerin) expression in *Igfbp2*$^{-/-}$ COBs (Fig. 3, *D* and *E*). The number of bone marrow adipocytes was reduced in PEG-HBD-treated *Igfbp2*$^{-/-}$ mice, although whole body adiposity was unchanged (Fig. 3*F* and supplemental Table S1). Not surprisingly, bone marrow *Ppar*γ expression was significantly reduced in COBs treated with PEG-HBD (Fig. 3*G*).

We previously reported that female *Igfbp2* $^{-/-}$ mice exhibited a different phenotype from male *Igfbp2*$^{-/-}$ mice in that no trabecular bone differences were noted in *Igfbp2*$^{-/-}$ female mice compared with littermate controls (10). Based on these observations, we analyzed whether PEG-HBD still had a positive effect on skeletal mass in female *Igfbp2*$^{-/-}$ mice even in the absence of a skeletal phenotype. At base line, whole body aBMD and aBMC/BW were not different between female *Igfbp2*$^{-/-}$ mice treated with PBS or PEG-HBD (supplemental Table S2). Interestingly, PEG-HBD significantly increased whole body

TABLE 4
MicroCT analysis of femurs from female *Igfbp2*$^{-/-}$ treated with PBS or PEG-HBD peptide
The values are expressed as the means ± S.E.

	Igfbp2$^{-/-}$	
	PBS (n = 10)	PEG-HBD (n = 4)
Midshaft		
Cortical thickness (mm)	0.176 ± 0.003	0.188 ± 0.003[a]
Bone area (mm^2)	0.726 ± 0.018	0.791 ± 0.012
Total area (mm^2)	1.744 ± 0.038	1.830 ± 0.039[b]
Bone area/total area	0.417 ± 0.006	0.433 ± 0.008
Distal femur		
Bone volume/total volume	0.038 ± 0.001	0.049 ± 0.006[c]
Trabecular number (1/mm)	2.99 ± 0.08	3.35 ± 0.12[c]
Trabecular thickness (mm)	0.035 ± 0.001	0.036 ± 0.002
Trabecular spacing (mm)	0.338 ± 0.011	0.298 ± 0.011[c]

[a] $p = 0.06$ *versus* *Igfbp2*$^{-/-}$ with PBS.
[b] $p = 0.05$ *versus* *Igfbp2*$^{-/-}$ with PBS.
[c] $p < 0.05$ *versus* *Igfbp2*$^{-/-}$ with PBS.

aBMD and aBMC/BW compared with PBS treatment (supplemental Table S2). MicroCT confirmed that the skeletal phenotype in response to PEG-HBD was very similar to what was observed in *Igfbp2*$^{-/-}$ males, *i.e.* enhanced cortical bone size and increased trabecular bone volume (Table 4). However, unlike the *Igfbp2*$^{-/-}$ male mice, the increase in trabecular volume fraction was associated with increased trabecular number rather than thickness. These lines of evidence imply that the HBD not only rescues the low bone mass phenotype of growing *Igfbp2*$^{-/-}$ male mice but also possesses an intrinsic anabolic effect during skeletal acquisition.

The Heparin-binding Domain of IGFBP-2 Suppresses PTEN Expression and Stimulates IGF-I/Akt Signaling—There is evidence of a negative association between IGFBP-2 and PTEN expression in human cancer cells such as glioblastoma and prostate cancer (19–21, 25). In addition, we have shown that PTEN expression was enhanced in *Igfbp2*-deficient osteoblasts (10). These findings led us to speculate that IGFBP-2 negatively regulates PTEN expression and enhances IGF-I signaling in osteoblasts. First, we analyzed whether IGFBP-2 suppressed PTEN expression using primary *Igfbp2*$^{-/-}$ COBs and found that full-length IGFBP-2 suppressed PTEN expression in these cells (Fig. 4, *A* and *B*). The control peptide had no effect on PTEN expression (Fig. 4, *C* and *D*), but much like IGFBP-2, the HBD peptide and PEG-HBD also induced a reduction in PTEN expression in a dose- and time-dependent manner (Fig. 4, *C–H*). Second, we asked whether the reduction in PTEN expression resulted in enhanced IGF-I/Akt signaling. Western blot analysis for phosphorylation of Akt at serine 473 (Ser(P)^{473}-Akt) revealed that IGF-I-stimulated Akt activation was impaired in *Igfbp2*$^{-/-}$ COBs compared with *Igfbp2*$^{+/+}$ COBs (Fig. 4, *I* and *J*). Furthermore, Ser(P)^{473}-Akt was enhanced in *Igfbp2*$^{-/-}$ COBs treated with PEG-HBD *versus* PBS-treated controls (Fig. 4, *K* and *L*). The effects of PEG-HBD on PTEN suppression and Akt phosphorylation by IGF-I were weaker than those of full-length IGFBP-2 protein (Fig. 4*M*). To examine which Akt isoform is involved in this process, we analyzed the expression of Akt1 and Akt2 in COBs. As shown in Fig. 4*N*, both Akt1 and Akt2 are expressed in this cell type. Interestingly, although Ser^{473} phosphorylation of Akt1 by IGF-I was impaired in *Igfbp2*$^{-/-}$ COBs, Akt2 phosphorylation by IGF-I was not changed after being adjusted by the expression of total Akt2 (Fig. 4*N*).

Finally, we investigated whether the heparin-binding domain of IGFBP-2 is required for the suppression of PTEN expression by IGFBP-2. For this purpose, we performed an *in vitro* binding assay to test whether IGFBP-2 can interact with COBs using biotinylated IGFBP-2 and found that IGFBP-2 binds to the cell surface of COBs, which was further enhanced in the presence of IGF-I (Fig. 4*O*). In addition, the binding of IGFBP-2 to the cell surface of COBs was partially blocked in the presence of PEG-HBD (Fig. 4*O*). These data indicate that IGFBP-2 enhances IGF-I-stimulated Akt activation by suppressing PTEN expression in part through its HBD, thereby further activating Akt1.

The Heparin-binding Domain of IGFBP-2 Stimulates IGF-I Induced Cytosolic β-Catenin Accumulation and Ser^{552} Phosphorylation of β-Catenin—Several lines of evidence demonstrate cross-talk between IGF-I signaling and β-catenin signaling in tumor cell lines (26–29). Thus, we hypothesized that IGF-I signaling would stimulate β-catenin signaling and that HBD peptide could enhance β-catenin signaling by suppressing PTEN expression in osteoblastic cells. We analyzed whether IGF-I affects β-catenin accumulation in the cytosol of osteoblastic cells. Western blot analysis revealed that IGF-I enhanced cytosolic accumulation of β-catenin associated with the reduced expression of membrane β-catenin in MC3T3-E1 cells (Fig. 5*A*). In addition, cytosolic accumulation of β-catenin in response to IGF-I was enhanced in *Igfbp2*$^{-/-}$ COBs treated with PEG-HBD compared with PBS-treated control cells (Fig. 5, *B* and *C*). This suggests that the HBD peptide is involved in IGF-I/β-catenin signaling possibly by suppressing PTEN expression. Ser^{552} phosphorylation of β-catenin, which can be induced by Akt, has been shown to be important for dissociation of β-catenin from membrane and relocalization to cytoplasm and nucleus (30–32). Based on this observation, we asked whether IGF-I stimulated Ser^{552} phosphorylation in β-catenin and whether the PEG-HBD facilitates this response in osteoblastic cells. As shown in Fig. 5 (*D–F*), IGF-I stimulated β-catenin phosphorylation on Ser^{552}, and this response was enhanced in cells treated with PEG-HBD. Because activation of β-catenin is important for bone formation, the osteogenic effect of the HBD peptide might be mediated by IGF-I/β-catenin signaling in osteoblasts (33).

DISCUSSION

In this study, we report that IGFBP-2 has anabolic properties in the growing skeleton and that part of its biologic effect is mediated through the HBD in an IGF binding-independent manner. IGFBP-2 levels are very high during neonatal growth and again during pubertal bone acquisition. IGF-I is also a critical factor for bone accrual, and it can induce IGFBP-2 expression in bone cells (34). Previous studies have shown that excess IGFBP-2 relative to IGF-I could inhibit the biologic activity of IGF-I (3). In line with this, an excess of IGFBP-2 has been shown to suppress osteoblast proliferation in part by antagonizing IGF-I action. *In vivo*, genetic models overexpressing *Igfbp2* have reduced body mass and bone size (7, 35). In contrast, Khosla and co-workers (8, 9) reported that IGF-II in complex with IGFBP-2 (used in equimolar amounts) had a high affinity for

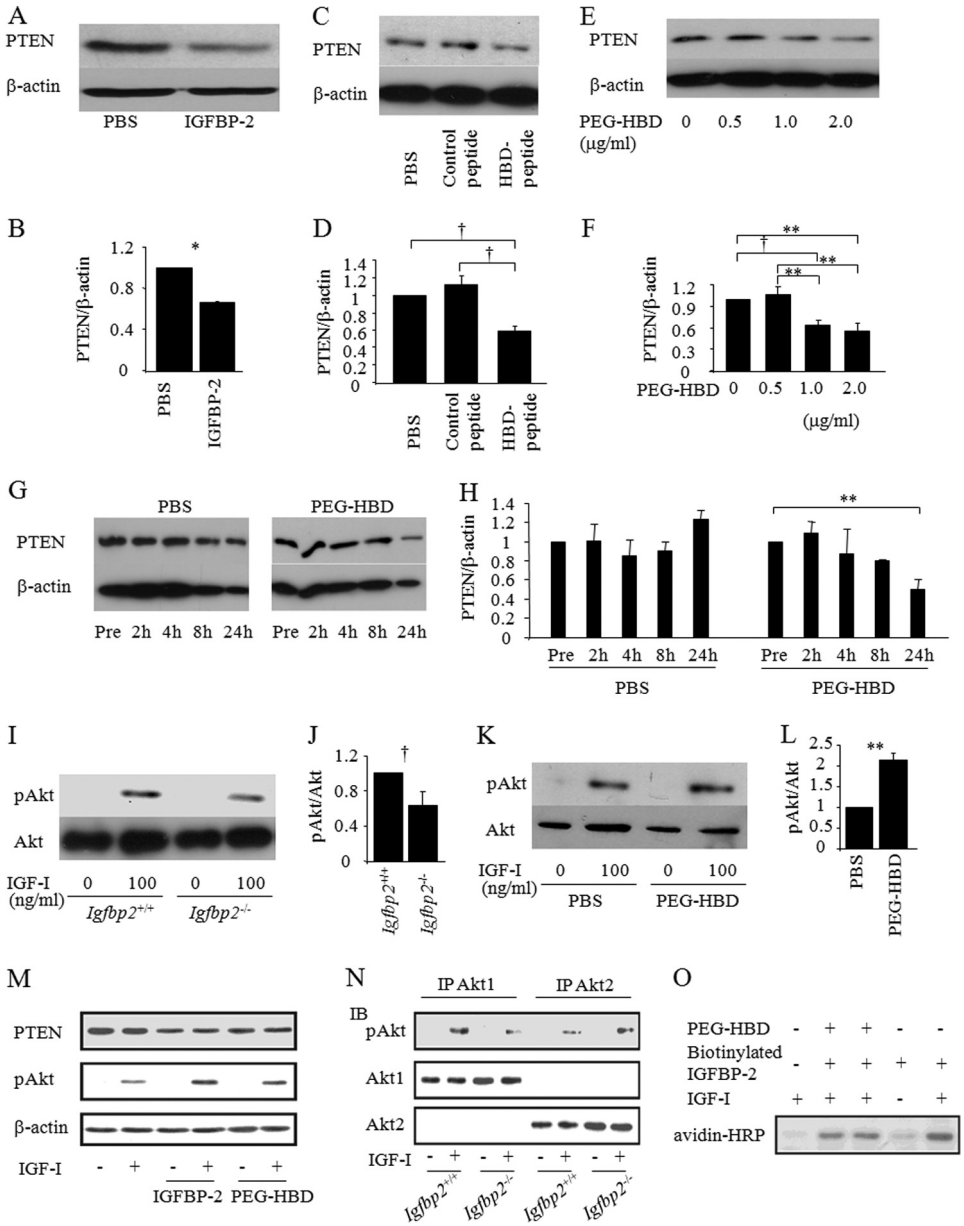

FIGURE 4. **The heparin-binding domain of IGFBP-2 suppresses PTEN expression.** *A* and *B*, *Igfbp2*$^{-/-}$ COBs were treated with PBS, control peptide, or HBD peptide overnight, and whole cell lysate was collected. PTEN expression was analyzed using Western blot analysis (*A*), and quantitative analysis was performed (*B*). *C–H*, *Igfbp2*$^{-/-}$ COBs were isolated and serum-starved overnight with PBS, IGFBP-2 (*C* and *D*) or PEG-HBD at the indicated concentration or period (*E–H*). Whole cell lysates were collected, and expression of PTEN was analyzed by Western blot analysis. Expression levels of PTEN were quantified by normalizing to the expression levels of β-actin. *I–L*, *Igfbp2*$^{+/+}$ or *Igfbp2*$^{-/-}$ COBs were serum-starved overnight and treated with IGF-I (100 ng/ml) for 15 min (*I* and *J*). *Igfbp2*$^{-/-}$ COBs were serum-starved with PBS or PEG-HBD overnight and treated with IGF-I (100 ng/ml) for 15 min (*K* and *L*). Whole cell lysates were collected, and expression of Ser(P)^{473}-Akt (*pAkt*) and Akt was analyzed by Western blot analysis. Expression levels of Ser(P)^{473}-Akt were quantified by normalizing to the expression levels of Akt. *M*, *Igfbp2*$^{-/-}$ COBs were exposed to IGF-I (50 ng/ml), IGFBP-2 (200 ng/ml), or the PEG-HBD (2 μg/ml) for 4 h. The lysates were prepared and immunoblotted for total PTEN or pAkt. Immunoblotting for β-actin is shown as a loading control. *N*, COBs were isolated from *Igfbp2*$^{+/+}$ and *Igfbp2*$^{-/-}$ mice. Duplicate cultures were exposed to IGF-I (50 ng/ml) for 10 min. The lysates were immunoprecipitated for Akt1 or Akt2 and then immunoblotted for pAkt or the respective Akt1 and Akt2 proteins. *O*, *Igfbp2*$^{-/-}$ COBs were incubated with IGF-I (50 ng/ml), IGFBP-2 (200 ng/ml), or the PEG-HBD (2 μg/ml) in the various combinations shown. They were also exposed to biotinylated IGFBP-2. Cell lysates were prepared and analyzed by SDS-PAGE with immunoblotting using HRP avidin. The figures shown represent at least three independent experiments. The values are expressed as the means ± S.E. ($n = 3–4$). *, $p < 0.001$; **, $p < 0.01$; †, $p < 0.05$; *IP*, immunoprecipitation; *IB*, immunoblot.

bone matrix, stimulated osteoblast proliferation, and could prevent disuse osteoporosis. Palermo *et al.* (34) also showed that lower concentrations of IGFBP-2-stimulated IGF-II induced *ALP* expression in rat tibial osteoblasts. In this study, we expand our insights into the physiologic role of IGFBP-2 and provide new evidence that the heparin-binding domain of IGFBP-2 may enhance bone mass principally by stimulating osteoblast proliferation.

Initially we characterized the skeletal phenotype of male *Igfbp2*$^{-/-}$ mice and found decreased skeletal mass, reduced numbers of osteoblasts, and low bone turnover (10). These findings suggested that physiological concentrations of IGFBP-2 were required for recruitment of osteoblasts and proper bone acquisition. Because forming a protein complex with IGFBP-2 is critical for stabilization of IGF-I in the pericel-

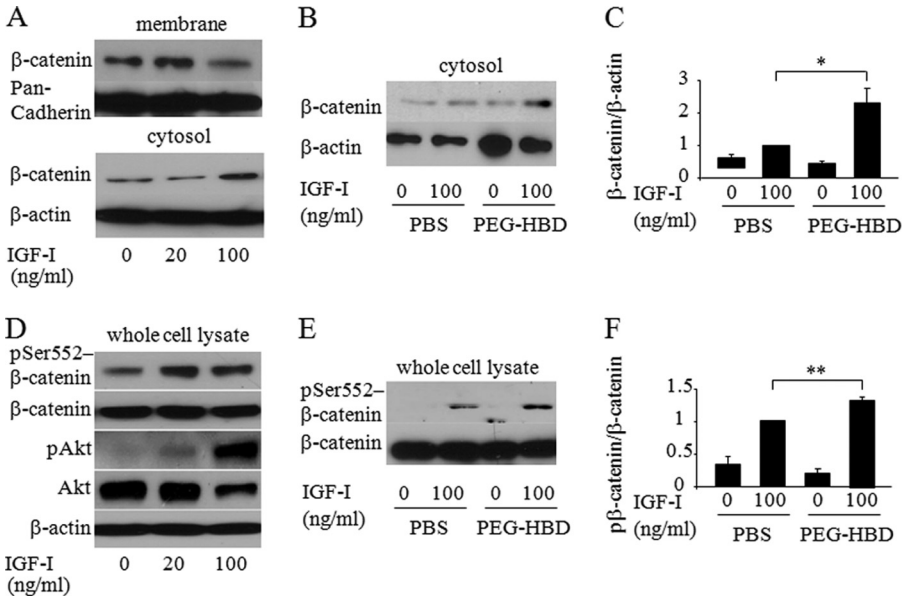

FIGURE 5. **The heparin-binding domain of IGFBP-2 stimulates cytosolic accumulation and Ser^{552} phosphorylation of β-catenin by IGF-I.** *A*, MC3T3-E1 cells were serum-starved overnight and treated with IGF-I at the indicated concentration for 6 h. Expression of β-catenin was analyzed by Western blot analysis using membrane and cytosolic fraction. Pan-cadherin and β-actin was used as a loading control for membrane and cytosolic fraction, respectively. *B* and *C*, *Igfbp2*$^{-/-}$ COBs were serum-starved overnight with PBS or PEG-HBD and treated with IGF-I (100 ng/ml) for 6 h. Expression of β-catenin was analyzed by Western blot analysis using cytosolic fraction (*B*) and quantified by normalizing to the expression levels of β-actin (*C*). *D*, MC3T3-E1 cells were serum-starved overnight and treated with IGF-I at the indicated concentration for 15 min. Expression of Ser(P)^{552}-β-catenin, β-catenin, Ser(P)^{473}-Akt (*pAkt*), and Akt was analyzed by Western blot analysis using whole cell lysates. *E* and *F*, *Igfbp2*$^{-/-}$ COBs were serum-starved overnight with PBS or PEG-HBD and treated with IGF-I (100 ng/ml) for 15 min. Expression of Ser(P)^{552}-β-catenin was analyzed by Western blot analysis using whole cell lysates (*E*) and quantified by normalizing to the expression levels of β-catenin (*F*). The figures shown represent at least three independent experiments. The values are expressed as the means ± S.E. ($n = 3$). *, $p < 0.01$; **, $p < 0.05$.

lular space, an anabolic action for IGFBP-2 was certainly conceivable, particularly when the anabolic effects of IGF-I were considered within that same context. Furthermore, emerging evidence suggests that IGFBP-2 could function at least partially independently of IGF-I binding to stimulate cell proliferation through the HBD domain that mediates IGFBP-2 binding to the extracellular matrix (13–16). Consistent with this tenet, we demonstrated that IGFBP-2 binding to the cell surface was partially blocked in the presence of the HBD peptide. Importantly, IGFBP-2 binding to the cell surface was greatly enhanced in the presence of IGF-I, suggesting that the native protein may have undergone a conformational change following IGF-I association.

Our finding that the HBD suppresses PTEN in osteoblasts and enhances osteoblast proliferation provides a possible mechanism by which IGFBP-2 could regulate skeletal mass, in coordination with IGF-I. This may be particularly relevant during stages of rapid bone growth such as the neonatal and adolescent period when the recruitment of osteoblast precursors is critical. However, sorting the IGF-I-dependent and independent activities of intact IGFBP-2 is challenging. Clearly, IGF-I signaling is a prerequisite for skeletal acquisition. Furthermore, we and others have shown that modulation of the IGF signaling pathway results in alterations in skeletal homeostasis (18, 36–41). Therefore, an anabolic effect of the HBD on the skeleton could in part be mediated by enhanced IGF-I-induced activation of the PI3K/Akt pathway as a result of PTEN suppression. In addition, the increase in osteoblast number in HBD-treated *Igfbp2*$^{-/-}$ mice could also be due to this mechanistic change because enhanced PI3K/Akt signaling in osteoblasts is involved in cell proliferation. In fact, Liu *et al.* (18) showed that the loss of PTEN in osteoblasts *in vivo* resulted in very high bone mass and increased osteoblast number.

Although administration of the HBD rescued the low osteoblast number in *Igfbp2*$^{-/-}$ mice, osteoclast number was further diminished by administration of HBD. This observation is consistent with the observed increase in bone mass but suggests that bone turnover is not accelerated by HBD treatment. Indeed, mineral apposition rate and bone formation rate showed minimal changes in *Igfbp2*$^{-/-}$ mice treated with HBD. In contrast to the HBD, IGF-I signaling has been shown to directly stimulate osteoclastogenesis (42), and our prior data suggest that physiological levels of IGFBP-2 in the skeletal microenvironment are required for osteoclastogenesis. It is very possible that IGFBP-2 acts to maintain IGF-I concentrations within the pericellular niche but that the HBD, which lacks the IGF-I-binding domain, may play a distinct role by inhibiting bone resorption when supraphysiologic concentrations are administered. Because the HBD does not directly suppress osteoclast differentiation *in vitro*, the underlying mechanism whereby the HBD decreases bone resorption is likely indirect and due to decreased *Rankl* expression in osteoblasts.

A reduction in PTEN expression has been shown to be associated with increased β-catenin signaling. Inactivation of GSK3β (glycogen synthase kinase 3) by Akt has been proposed to be the key pathway by which Akt activation enhances β-catenin stabilization, whereas several lines of evidence demonstrate the important role of Ser^{552} phosphorylation in β-catenin activation (30–32). β-Catenin is directly phosphorylated by Akt, and Ser^{552} phosphorylation is important for cyto-

solic and nuclear accumulation of β-catenin, resulting in increased β-catenin transcriptional activity (30). He *et al.* (18) reported that the loss of PTEN resulted in an excess of intestinal stem cells by stimulating β-catenin activity in part through Ser^{552} phosphorylation (31). In the current study, we demonstrated that IGF-I enhanced β-catenin accumulation in cytoplasm and phosphorylated Ser^{552} of β-catenin in osteoblastic cells, and this response was further enhanced by addition of the HBD. Taken together, these lines of evidence support our findings of a synergistic effect of IGFBP-2 with IGF-I on β-catenin signaling and suggest that the increased bone formation noted in *Igfbp2*$^{-/-}$ mice treated with PEG-HBD is related to activation of this signaling pathway.

In the PEG-HBD-treated *Igfbp2*$^{-/-}$ mice, cell proliferation (as measured by BrdUrd labeling) and osteoblast number by histomorphometry were increased and were accompanied by reduced number of marrow adipocytes. Mesenchymal cell allocation is an important step in regulating bone mass and marrow adiposity. Numerous factors are involved in this process including Wnt/β-catenin signaling and the transcription factor, PPAR-γ (43). Activation of Wnt/β-catenin signaling favors osteoblastogenesis over adipogenesis in part by either sequestering PPAR-γ or suppressing PPAR-γ transcriptional activity (44–46). Because HBD enhances β-catenin stability that is induced by IGF-I, the switch of mesenchymal cells toward the osteogenic lineage might explain the increased cell proliferation as well as osteoblast number and reduced adipocyte number in bone marrow from *Igfbp2*$^{-/-}$ mice treated with PEG-HBD.

Nevertheless, the mechanism by which the HBD suppresses PTEN expression has not been defined. One possibility resides in the binding of HBD with the integrin receptor. Maile *et al.* (47) reported that heparin-binding domain of vitronectin bound to a cysteine loop region of β3 integrin and modulated αVβ3 integrin signaling in smooth muscle cells. Furthermore, Perks *et al.* (20) reported that PTEN down-regulation by IGFBP-2 might be mediated by an integrin receptor, although they did not demonstrate an interaction between IGFBP-2 and a specific integrin receptor or whether the HBD was involved in this interaction. Further studies are needed to define specific sites of IGFBP-2 binding leading to activation of two critical intracellular signaling pathways.

Our results using supraphysiologic concentration of the HBD cannot be used to reach a definitive conclusion regarding the role of physiologic concentrations of IGFBP-2 in bone acquisition, particularly relative to IGF-I. However, it does suggest that this binding protein has unique properties that might explain the high circulating levels of IGFBP-2 during periods of rapid growth such as the first year of life and during puberty, a time when serum IGF-I levels are also high. Importantly, HBD increased bone mass even in growing female mice that do not have alterations in bone mineral density (10). Further analyses are needed to determine whether HBD also has an anabolic effect in older mice. Notwithstanding, we found that the HBD in IGFBP-2 has an anabolic effect on the skeleton of growing mice by targeting osteoblast recruitment through suppression of PTEN expression and activation of β-catenin signaling. These data support the tenet that IGFBP-2, which is induced by IGF-I, could act synergistically with IGF-I to promote cell proliferation through its unique heparin-binding domain in the linker region of the molecule. Our studies lend further support to recent work from the Lodish laboratory (11) demonstrating the strong proliferative properties of IGFBP-2 in hematopoietic stem cells and provide a potential mechanism for IGFBP-2 activity in some neoplasms.

In summary, we show that the HBD in IGFBP-2 has an anabolic effect on the skeleton, and this effect is mediated by the suppression of PTEN expression and involves activation of β-catenin signaling. These lines of evidence add to our growing knowledge regarding the physiologic role of IGFBP-2 relative to IGF-I in several tissues and provide insights into the cross-talk between two signaling networks that have been shown to be essential for bone growth and maintenance.

REFERENCES

1. Hwa, V., Oh, Y., and Rosenfeld, R. G. (1999) *Endocr. Rev.* **20,** 761–787
2. Jones, J. I., and Clemmons, D. R. (1995) *Endocr. Rev.* **16,** 3–34
3. Firth, S. M., and Baxter, R. C. (2002) *Endocr. Rev.* **23,** 824–854
4. Hu, D., Pawlikowska, L., Kanaya, A., Hsueh, W. C., Colbert, L., Newman, A. B., Satterfield, S., Rosen, C., Cummings, S. R., Harris, T. B., and Ziv, E. (2009) *J. Am. Geriatr. Soc.* **57,** 1213–1218
5. Hedbacker, K., Birsoy, K., Wysocki, R. W., Asilmaz, E., Ahima, R. S., Farooqi, I. S., and Friedman, J. M. (2010) *Cell Metab.* **11,** 11–22
6. Wheatcroft, S. B., Kearney, M. T., Shah, A. M., Ezzat, V. A., Miell, J. R., Modo, M., Williams, S. C., Cawthorn, W. P., Medina-Gomez, G., Vidal-Puig, A., Sethi, J. K., and Crossey, P. A. (2007) *Diabetes* **56,** 285–294
7. Hoeflich, A., Nedbal, S., Blum, W. F., Erhard, M., Lahm, H., Brem, G., Kolb, H. J., Wanke, R., and Wolf, E. (2001) *Endocrinology* **142,** 1889–1898
8. Conover, C. A., Johnstone, E. W., Turner, R. T., Evans, G. L., John Ballard, F. J., Doran, P. M., and Khosla, S. (2002) *Growth Horm. IGF Res.* **12,** 178–183
9. Khosla, S., Hassoun, A. A., Baker, B. K., Liu, F., Zein, N. N., Whyte, M. P., Reasner, C. A., Nippoldt, T. B., Tiegs, R. D., Hintz, R. L., and Conover, C. A. (1998) *J. Clin. Invest.* **101,** 2165–2173
10. DeMambro, V. E., Clemmons, D. R., Horton, L. G., Bouxsein, M. L., Wood, T. L., Beamer, W. G., Canalis, E., and Rosen, C. J. (2008) *Endocrinology* **149,** 2051–2061
11. Zhang, C. C., Kaba, M., Iizuka, S., Huynh, H., and Lodish, H. F. (2008) *Blood* **111,** 3415–3423
12. Arai, T., Busby, W., Jr., and Clemmons, D. R. (1996) *Endocrinology* **137,** 4571–4575
13. Russo, V. C., Bach, L. A., Fosang, A. J., Baker, N. L., and Werther, G. A. (1997) *Endocrinology* **138,** 4858–4867
14. Russo, V. C., Rekaris, G., Baker, N. L., Bach, L. A., and Werther, G. A. (1999) *Endocrinology* **140,** 3082–3090
15. Russo, V. C., Schütt, B. S., Andaloro, E., Ymer, S. I., Hoeflich, A., Ranke, M. B., Bach, L. A., and Werther, G. A. (2005) *Endocrinology* **146,** 4445–4455
16. Duan, C., Ding, J., Li, Q., Tsai, W., and Pozios, K. (1999) *Proc. Natl. Acad. Sci. U.S.A.* **96,** 15274–15279
17. Kawai, M., and Rosen, C. J. (2009) *Pediatr. Nephrol.* **24,** 1277–1285
18. Liu, X., Bruxvoort, K. J., Zylstra, C. R., Liu, J., Cichowski, R., Faugere, M. C., Bouxsein, M. L., Wan, C., Williams, B. O., and Clemens, T. L. (2007) *Proc. Natl. Acad. Sci. U.S.A.* **104,** 2259–2264
19. Mehrian-Shai, R., Chen, C. D., Shi, T., Horvath, S., Nelson, S. F., Reichardt, J. K., and Sawyers, C. L. (2007) *Proc. Natl. Acad. Sci. U.S.A.* **104,** 5563–5568
20. Perks, C. M., Vernon, E. G., Rosendahl, A. H., Tonge, D., and Holly, J. M. (2007) *Oncogene* **26,** 5966–5972
21. Levitt, R. J., Georgescu, M. M., and Pollak, M. (2005) *Biochem. Biophys. Res. Commun.* **336,** 1056–1061
22. Sakata, T., Wang, Y., Halloran, B. P., Elalieh, H. Z., Cao, J., and Bikle, D. D. (2004) *J. Bone Miner. Res* **19,** 436–446

23. Shoba, L. N., and Lee, J. C. (2003) *J. Cell. Biochem.* **88,** 1247–1255
24. Wood, T. L., Rogler, L. E., Czick, M. E., Schuller, A. G., and Pintar, J. E. (2000) *Mol. Endocrinol.* **14,** 1472–1482
25. Cohen, P., Peehl, D. M., Stamey, T. A., Wilson, K. F., Clemmons, D. R., and Rosenfeld, R. G. (1993) *J. Clin. Endocrinol. Metab.* **76,** 1031–1035
26. Jin, T., George Fantus, I., and Sun, J. (2008) *Cell Signal.* **20,** 1697–1704
27. Desbois-Mouthon, C., Cadoret, A., Blivet-Van Eggelpoël, M. J., Bertrand, F., Cherqui, G., Perret, C., and Capeau, J. (2001) *Oncogene* **20,** 252–259
28. Playford, M. P., Bicknell, D., Bodmer, W. F., and Macaulay, V. M. (2000) *Proc. Natl. Acad. Sci. U.S.A.* **97,** 12103–12108
29. Amin, S., Riggs, B. L., Melton, L. J., 3rd, Achenbach, S. J., Atkinson, E. J., and Khosla, S. (2007) *J. Bone Miner. Res.* **22,** 799–807
30. Fang, D., Hawke, D., Zheng, Y., Xia, Y., Meisenhelder, J., Nika, H., Mills, G. B., Kobayashi, R., Hunter, T., and Lu, Z. (2007) *J. Biol. Chem.* **282,** 11221–11229
31. He, X. C., Yin, T., Grindley, J. C., Tian, Q., Sato, T., Tao, W. A., Dirisina, R., Porter-Westpfahl, K. S., Hembree, M., Johnson, T., Wiedemann, L. M., Barrett, T. A., Hood, L., Wu, H., and Li, L. (2007) *Nat. Genet.* **39,** 189–198
32. Taurin, S., Sandbo, N., Qin, Y., Browning, D., and Dulin, N. O. (2006) *J. Biol. Chem.* **281,** 9971–9976
33. Glass, D. A., 2nd, and Karsenty, G. (2006) *Curr. Top. Dev. Biol.* **73,** 43–84
34. Palermo, C., Manduca, P., Gazzerro, E., Foppiani, L., Segat, D., and Barreca, A. (2004) *Am. J. Physiol. Endocrinol. Metab.* **286,** E648–E657
35. Eckstein, F., Pavicic, T., Nedbal, S., Schmidt, C., Wehr, U., Rambeck, W., Wolf, E., and Hoeflich, A. (2002) *Anat. Embryol.* **206,** 139–148
36. Fujita, T., Azuma, Y., Fukuyama, R., Hattori, Y., Yoshida, C., Koida, M., Ogita, K., and Komori, T. (2004) *J. Cell Biol.* **166,** 85–95
37. Peng, X. D., Xu, P. Z., Chen, M. L., Hahn-Windgassen, A., Skeen, J., Jacobs, J., Sundararajan, D., Chen, W. S., Crawford, S. E., Coleman, K. G., and Hay, N. (2003) *Genes Dev.* **17,** 1352–1365
38. Liu, J. P., Baker, J., Perkins, A. S., Robertson, E. J., and Efstratiadis, A. (1993) *Cell* **75,** 59–72
39. Yakar, S., Rosen, C. J., Beamer, W. G., Ackert-Bicknell, C. L., Wu, Y., Liu, J. L., Ooi, G. T., Setser, J., Frystyk, J., Boisclair, Y. R., and LeRoith, D. (2002) *J. Clin. Invest.* **110,** 771–781
40. Zhang, M., Xuan, S., Bouxsein, M. L., von Stechow, D., Akeno, N., Faugere, M. C., Malluche, H., Zhao, G., Rosen, C. J., Efstratiadis, A., and Clemens, T. L. (2002) *J. Biol. Chem.* **277,** 44005–44012
41. Zhao, G., Monier-Faugere, M. C., Langub, M. C., Geng, Z., Nakayama, T., Pike, J. W., Chernausek, S. D., Rosen, C. J., Donahue, L. R., Malluche, H. H., Fagin, J. A., and Clemens, T. L. (2000) *Endocrinology* **141,** 2674–2682
42. Wang, Y., Nishida, S., Elalieh, H. Z., Long, R. K., Halloran, B. P., and Bikle, D. D. (2006) *J. Bone Miner. Res.* **21,** 1350–1358
43. Gesta, S., Tseng, Y. H., and Kahn, C. R. (2007) *Cell* **131,** 242–256
44. Liu, J., Wang, H., Zuo, Y., and Farmer, S. R. (2006) *Mol. Cell. Biol.* **26,** 5827–5837
45. Bennett, C. N., Longo, K. A., Wright, W. S., Suva, L. J., Lane, T. F., Hankenson, K. D., and MacDougald, O. A. (2005) *Proc. Natl. Acad. Sci. U.S.A.* **102,** 3324–3329
46. Ross, S. E., Hemati, N., Longo, K. A., Bennett, C. N., Lucas, P. C., Erickson, R. L., and MacDougald, O. A. (2000) *Science* **289,** 950–953
47. Maile, L. A., Aday, A. W., Busby, W. H., Sanghani, R., Veluvolu, U., and Clemmons, D. R. (2008) *J. Cell. Biochem.* **105,** 437–446